A fotoionizáció spektroszkópiai alkalmazásai

1) Bevezetés: alapjelenség és alapelvek

2) Fotoelektron-spektroszkópia (UPS, XPS)

3) A kísérleti berendezés

4) A fotoelektron (pe) spektrum

5) Sávszerkezet

   - Rezgési szerkezet
   - Spin-pálya csatolás
   - Jahn-Teller effektus
   - Disszociáció
   - Autoionizáció
   - Nyílthéjú rendszerek

6) A pe spektrumok értelmezése

7) Kémiai alkalmazások

8) A fotoionizációs tömegspektrometria

9) Fotoelektron-fotoion-koincidencia (PEPICO)

10) Zérus kinetikus energia(jú elektronok analízisén alapuló) spektroszkópia (ZEKE)

11) Röntgengerjesztéses fotoelektron-spektroszkópia (XPS)

Bevezetés

1) A fotoelektromos hatás

Phillip vonLenard (1902):"The number of electrons depended on the intensity of light and not its colour."
Albert Einstein: the law of the photoelectric effect (1905)
Noble Prize (1921)

2) Történeti áttekintés (UPS, XPS)

3) Gerjesztési és ionizációs folyamatok, ionizáló részecskék

4) A küszöbtörvény

5) Ionizációs mechanizmusok

6) A pe spektrum kialakulása

7) A keletkezett ionok „sorsa"

8) Fotoionizációs hatáskeresztmetszet

9) *Franck-Condon*-elv

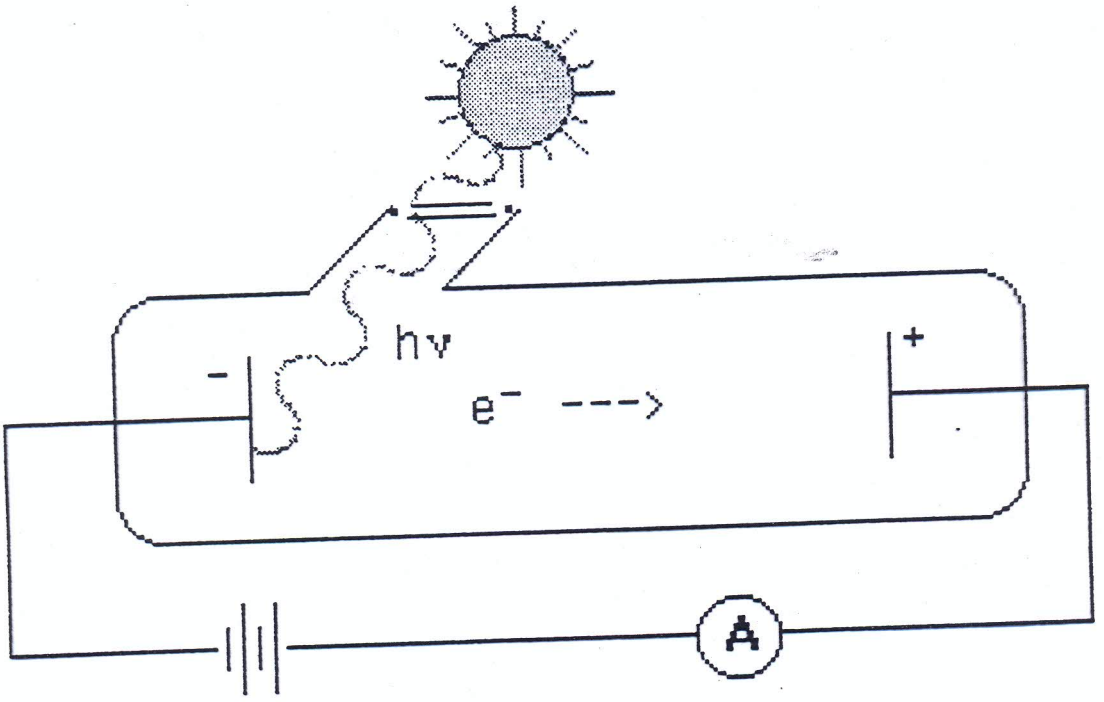
hν
e⁻ --->
-
+
A

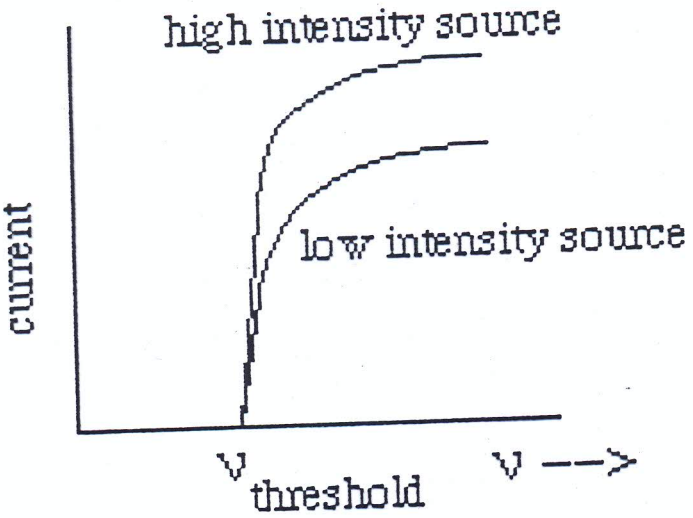
high intensity source
low intensity source
current
V threshold
V -->

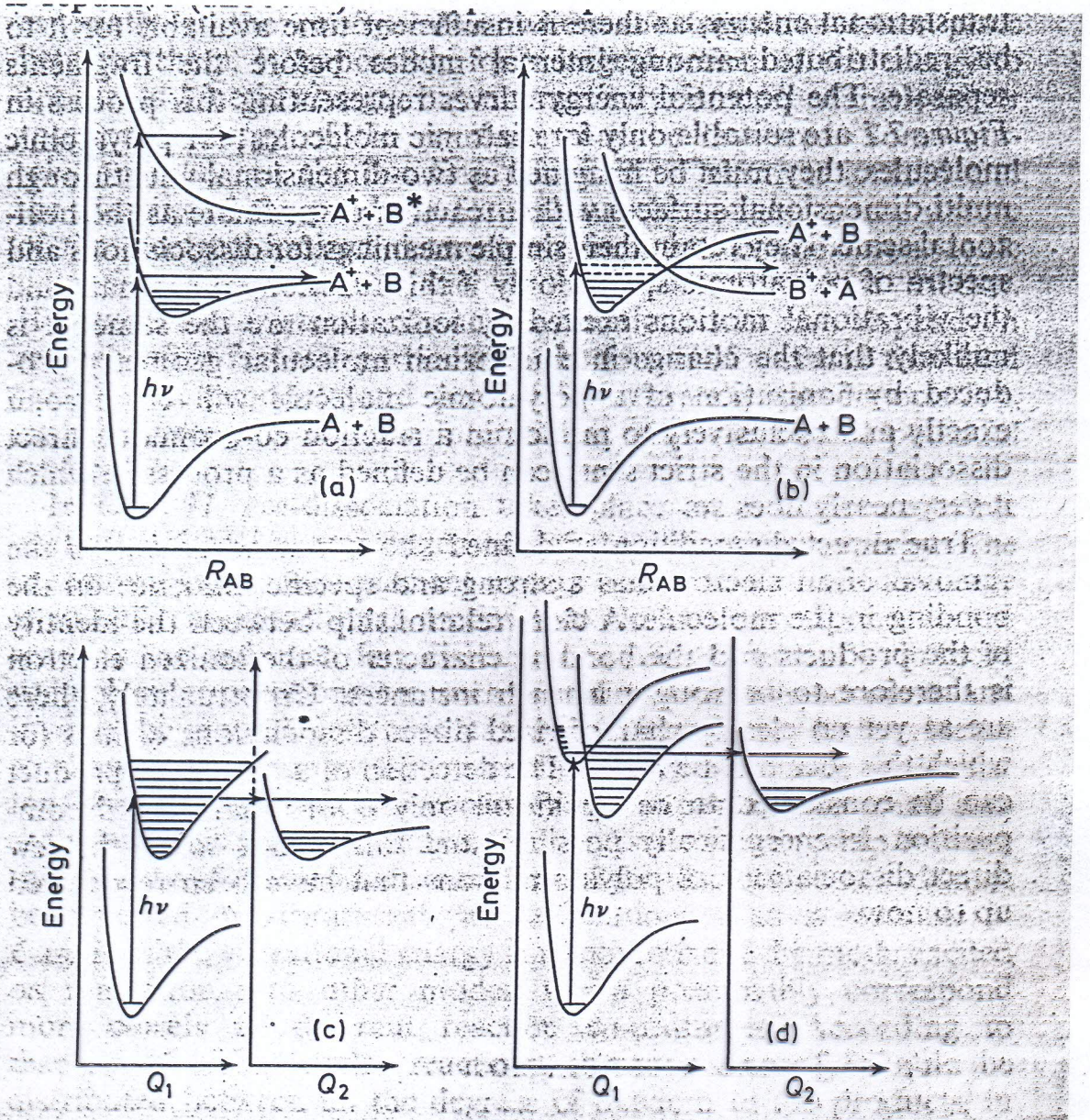

Figure 7.1. Potential energy curves illustrating some important dissociation mechanisms: (a) direct dissociation; (b) electronic pre-dissociation; (c) vibrational pre-dissociation; (d) internal conversion with vibrational pre-dissociation. In (c) and (d) the co-ordinates Q_1 and Q_2 represent different molecular motions in a polyatomic molecule

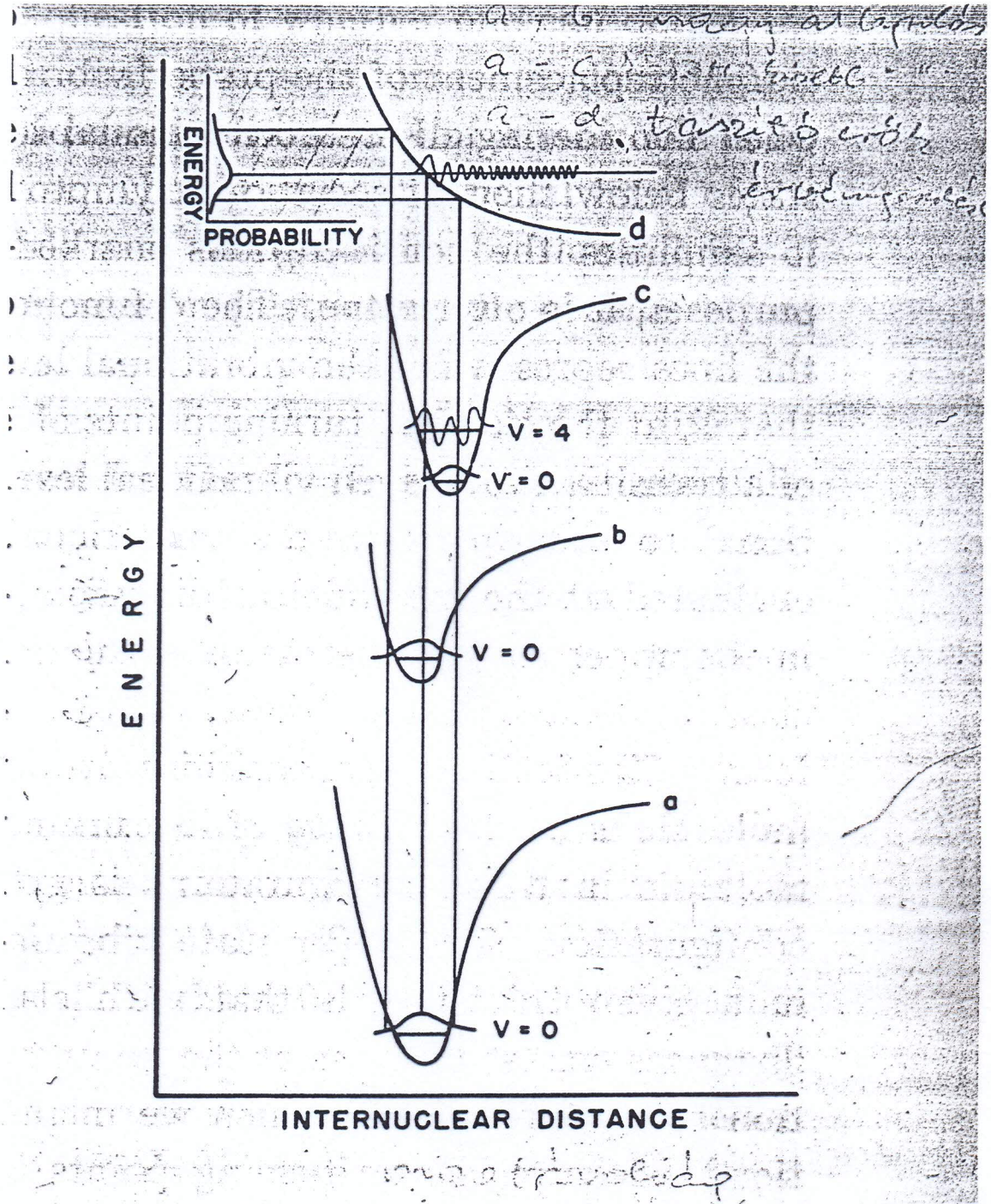

FIG. 21. Illustrative diatomic molecule and molecule-ion potential energy curves. The actual energy difference between curves a and b, c, and d is much greater than represented.

$$FCF = |\langle \chi_{v'} | \chi_{v''} \rangle|^2$$

$\chi_{v''}$ = vibr. wave funct. in the M

$\chi_{v'}$ = vibr. wavefunct. in the M^+

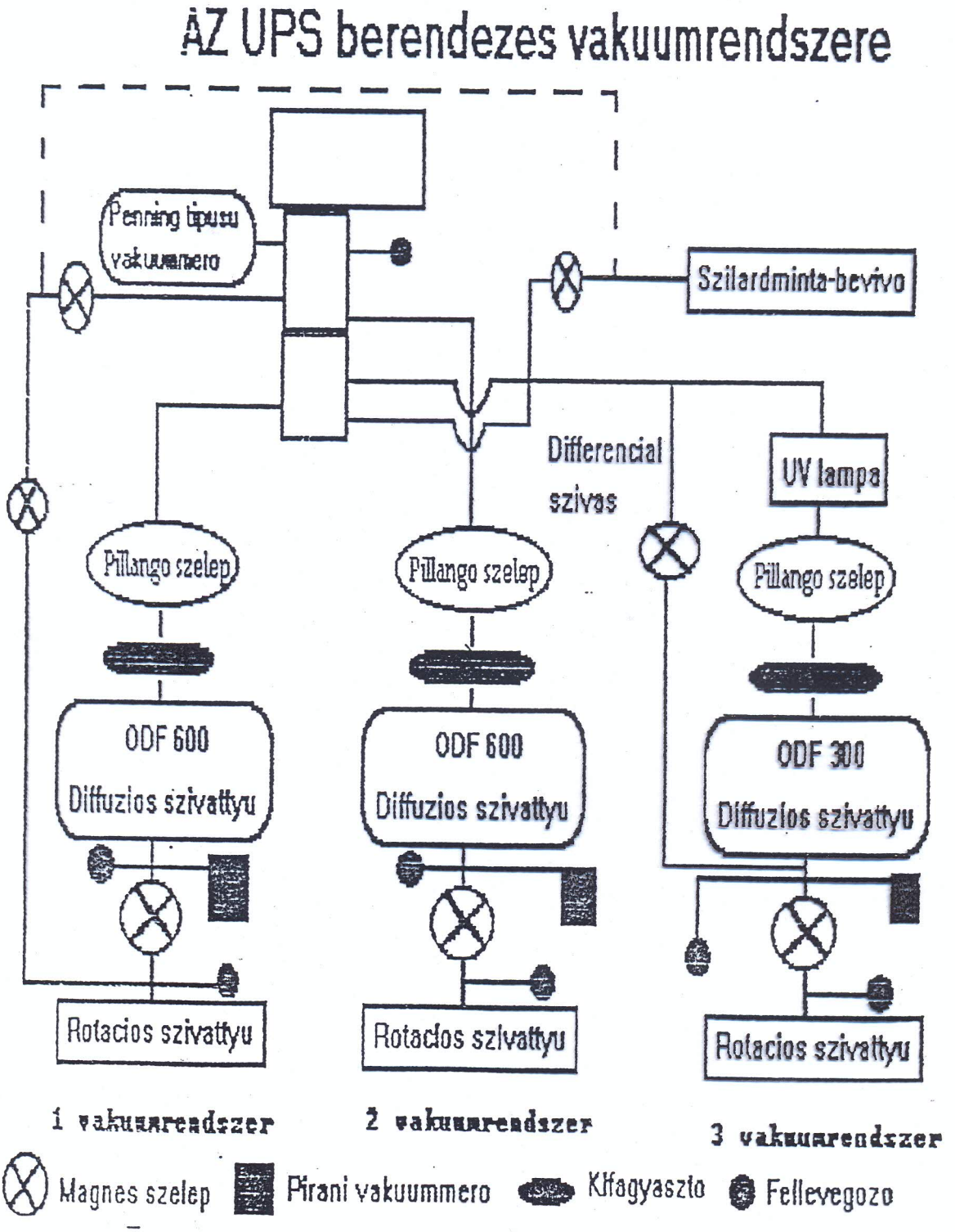
AZ UPS berendezes vakuumrendszere
Penning tipusu vakuummero
Szilardminta-bevivo
Differencial szivas
UV lampa
Pillango szelep
Pillango szelep
Pillango szelep
ODF 600
Diffuzios szivattyu
ODF 600
Diffuzios szivattyu
ODF 300
Diffuzios szivattyu
Rotacios szivattyu
Rotacios szivattyu
Rotacios szivattyu
1 vakuumrendszer
2 vakuumrendszer
3 vakuumrendszer
Magnes szelep
Pirani vakuummero
Kifagyaszto
Fellevegozo

2. ábra

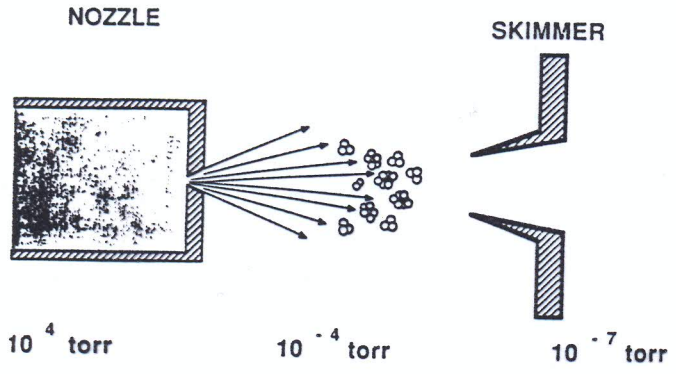

Figure 2. Illustration of the supersonic expansion method of synthesizing beams of atomic clusters. See text for description.

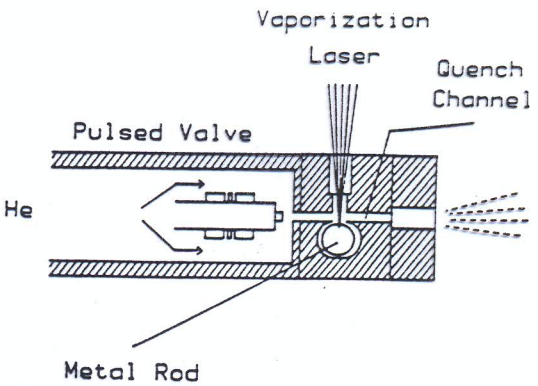

Figure 3. Illustration of the laser vaporization flow condensation method for synthesis of meal or semi-metal clusters. The pulsed gas valve is placed in a high-vacuum chamber, and synchronous pulses from a focused laser beam repeatedly irradiate the rotating target. At right, the gas jet expands into vacuum. (Adapted from Reference 35.)

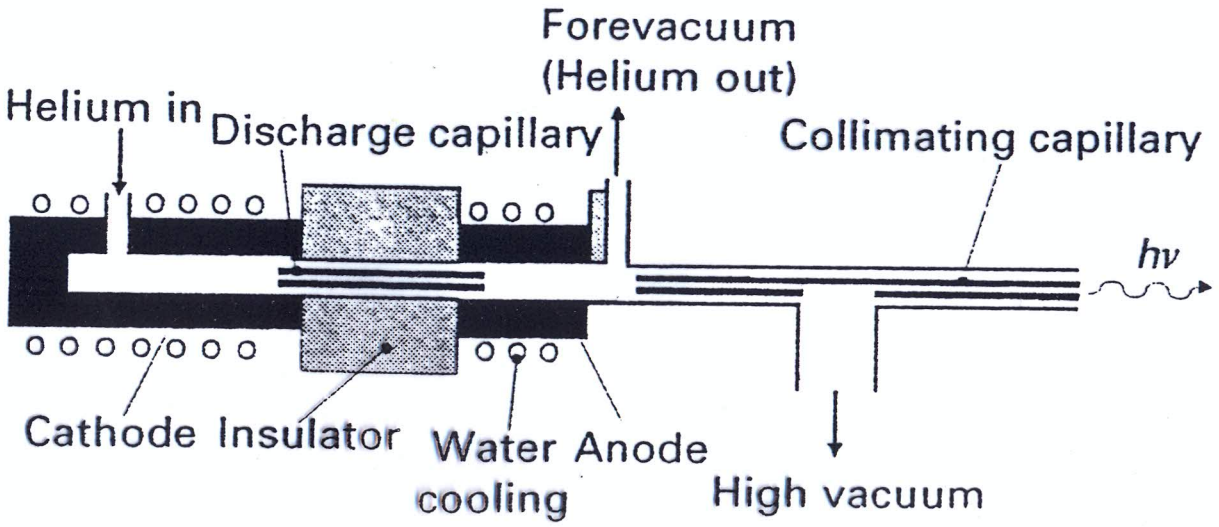

Figure 3 Low-pressure helium d.c. discharge lamp.

Vonal	energia eV	hullámhossz nm	rel. intenzitás
He Iα	**21,2175**	**58,43340**	**100**
He Iβ	23,0865	53,70296	2
He Iγ	23,7415	52,22128	0,5
He IIα	**40,8136**	**30,3781**	**100**
He IIβ	48,3702	25,6317	5
He IIγ	51,0153	24,3027	
He IIδ	52,2397	23,7331	
H Lyman α	10,1986	121,567	100
H Lyman β	12,0872	102,57	10
H Lyman γ	12,7482	97,25	1
Ne Iα	16,6704 16,8476	74,36 73,5895	15 100

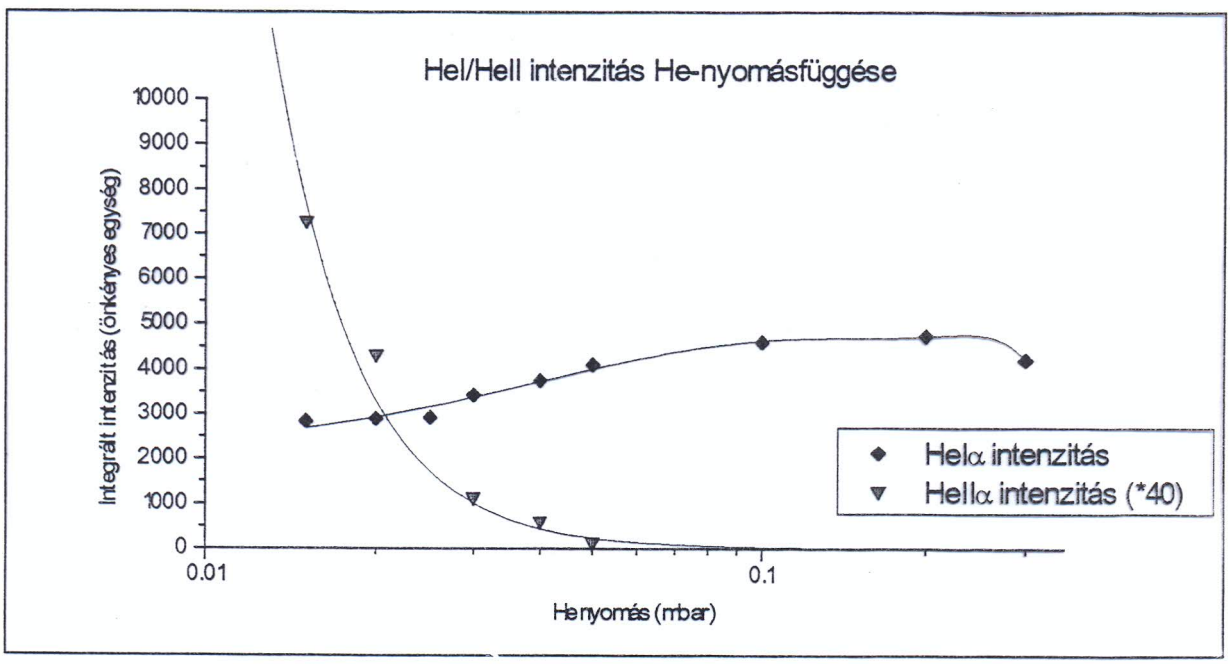

Ar $^2P_{3/2}$ ionizáció

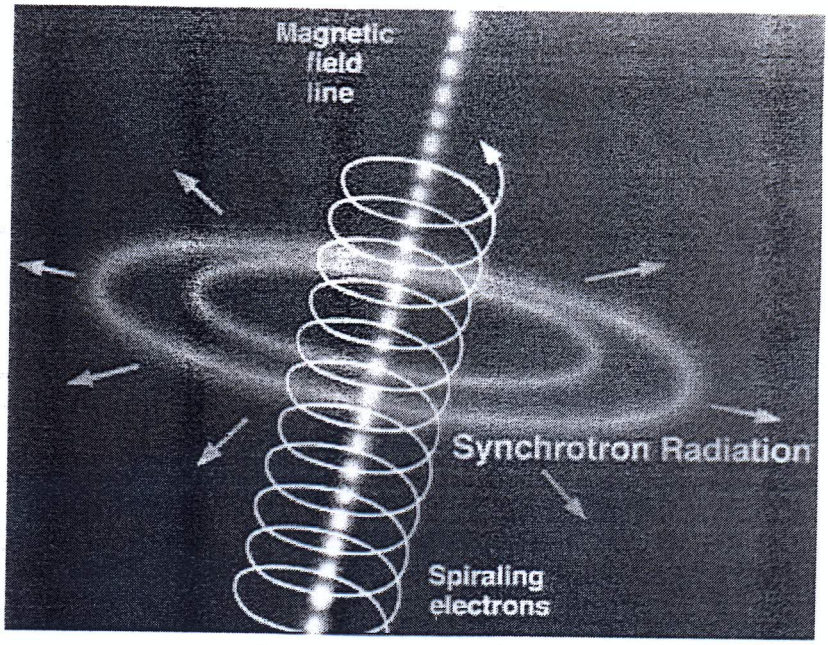
Magnetic field line
Synchrotron Radiation
Spiraling electrons

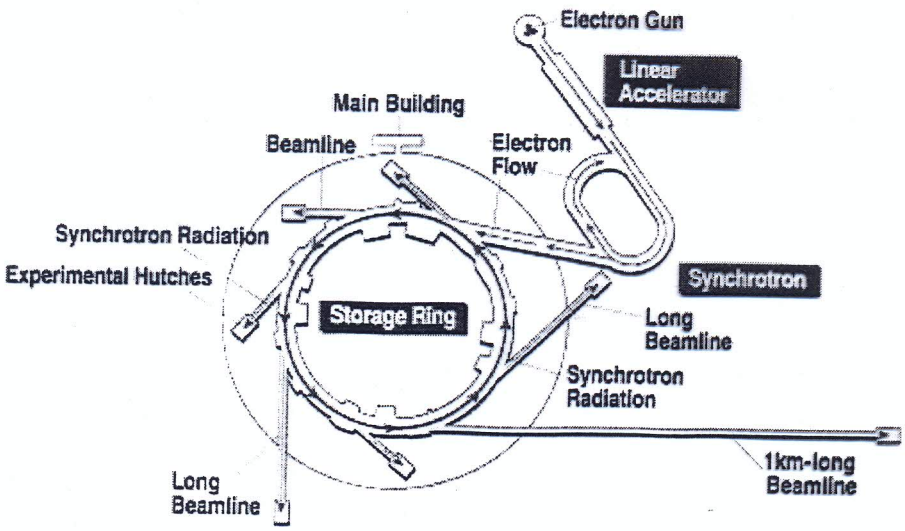
Electron Gun
Linear Accelerator
Main Building
Beamline
Electron Flow
Synchrotron Radiation
Experimental Hutches
Storage Ring
Synchrotron
Long Beamline
Synchrotron Radiation
1km-long Beamline
Long Beamline

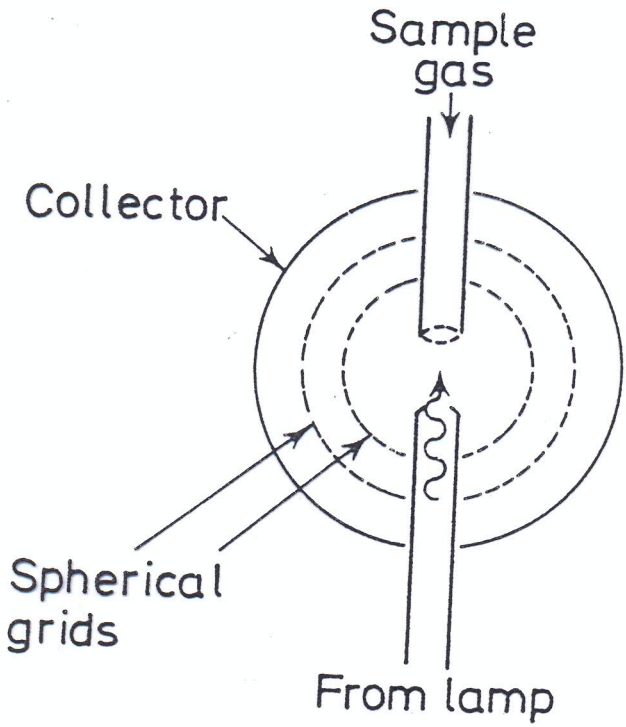

(c)

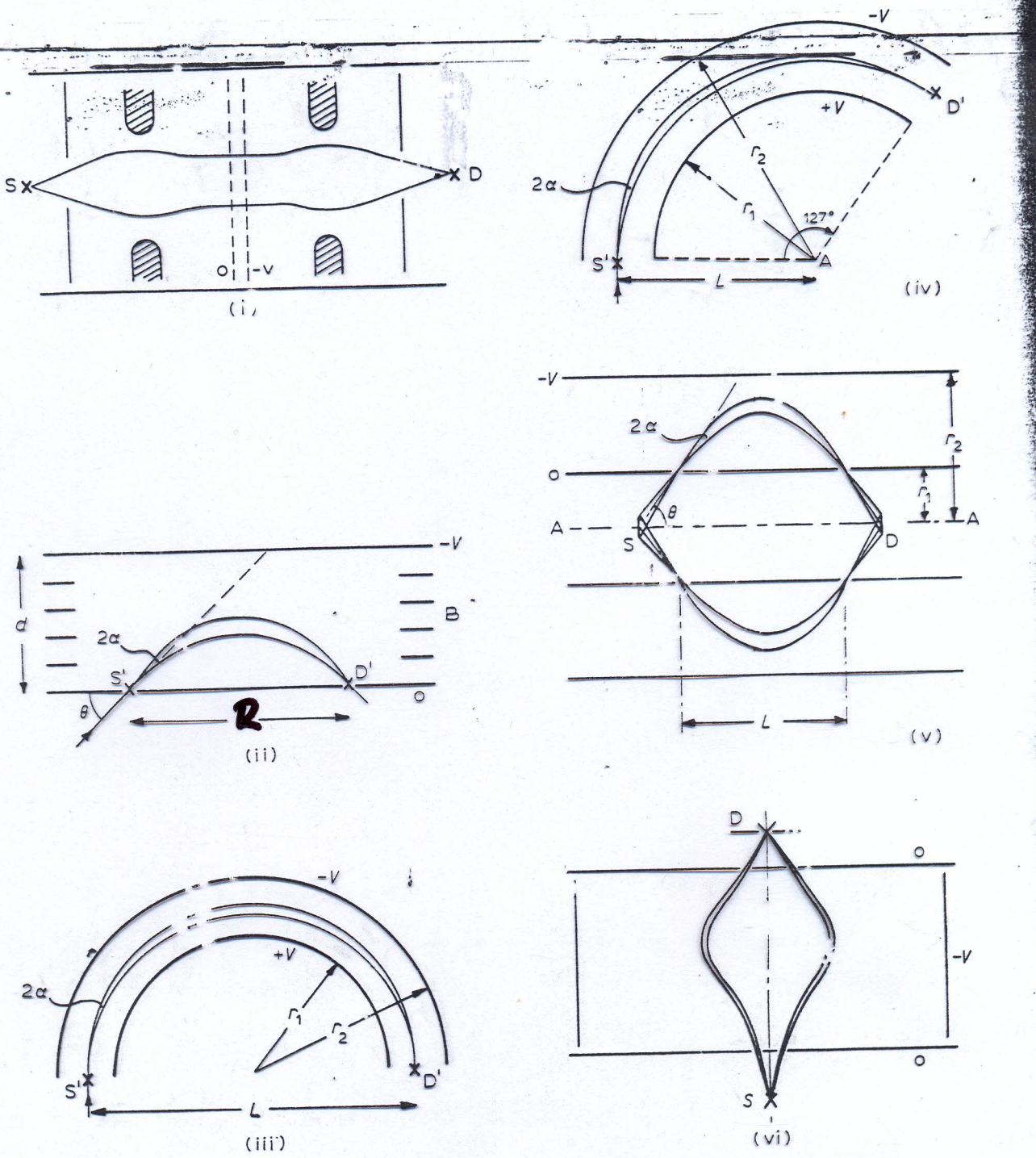

Fig. 14. Electrostatic energy analysers. The dimensions shown on the diagrams define the quantities used for the calculation of the properties of the analysers (see text). (i) Retarding field analyser (cylindrically symmetric about axis SD). (ii) Parallel plate analyser. (iii) Hemispherical analyser (spherically symmetric). (iv) 127° cylindrical analyser (cylindrically symmetric about perpendicular axis through A). (v) Cylindrical mirror (cylindrically symmetric about axis AA). (vi) Allen Bessel box [100] (cylindrically symmetric about axis SD).

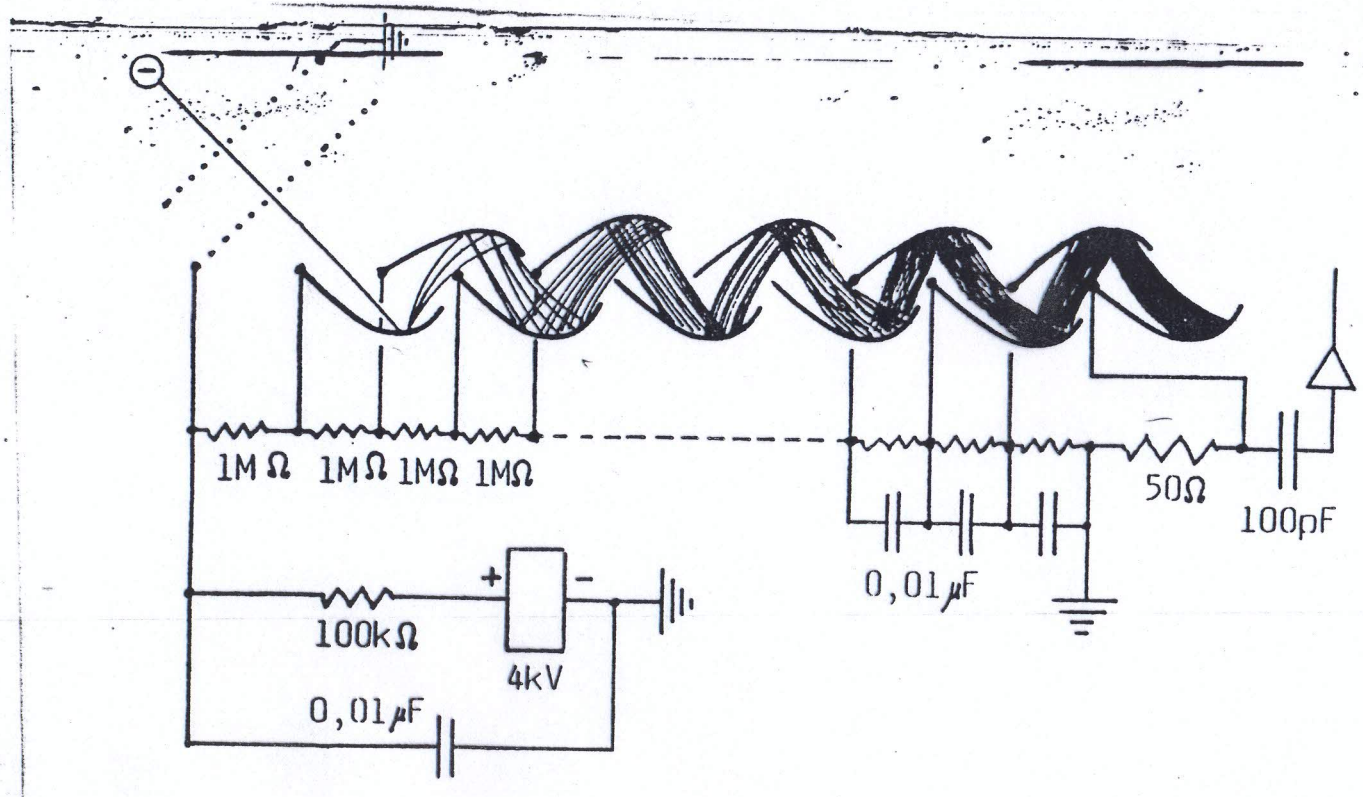

Elektronsokszorozó. Az ábrán látható bekötésben elektronok, vagy negatív töltésű részecskék detektálására alkalmas.

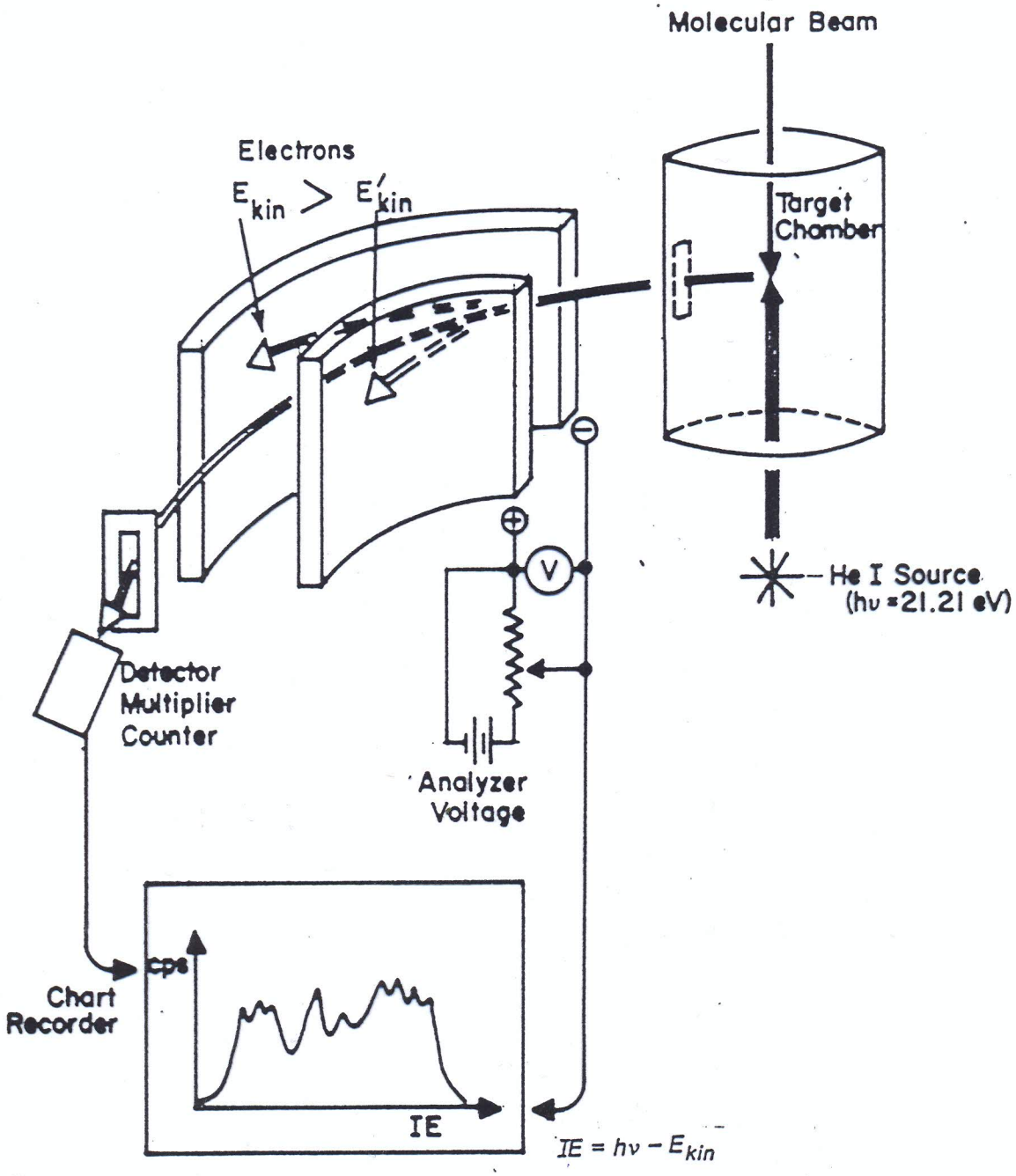

Figure 2. Schematic diagram of a low energy photoelectron spectrometer.

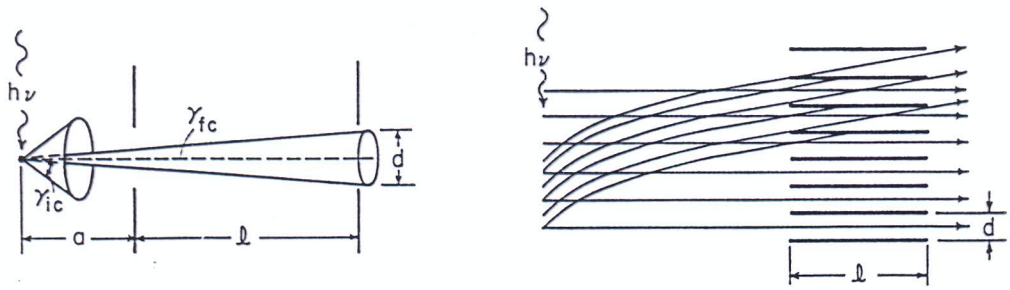

3 Two types of threshold electron energy analyzers. An idealized analyzer with a ıization source is shown in (a) in which γ_{ic} is the initial planar angle of electron ejection he final planar angle after acceleration. An analyzer useful for extended ionization s shown in (b). The long pipes, available commercially as collimated hole structures, ıate against electrons with significant perpendicular velocity components.

$\gamma_{fc} = 0{,}5d/(\ell+2a)$ $\quad (\ell/d) = 10-50$

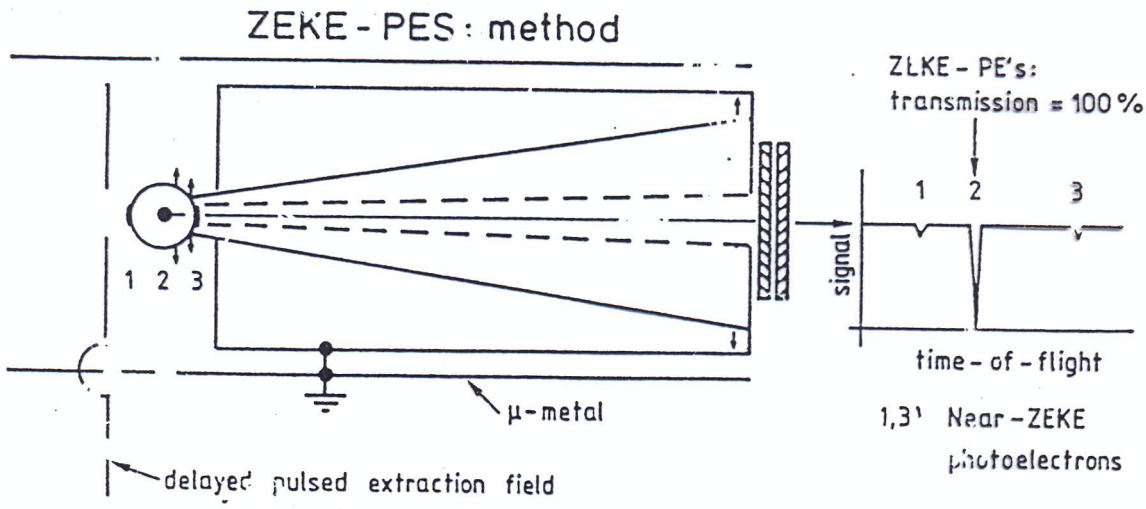

Figure 3 Princi[illegible] of ZEKE photoelectron detection and discrimi[illegible]ion against near-ZEKE electrons. In the example, a field-free delay of 1 μs and a kinetic energy of 0.1 meV ($v = 6$ mm/μs) is chosen for the near-ZEKE electrons 1 and 3. The electrons 1, 3 are discriminated against the ZEKE electron 2 by their TOF. The off-axis near-ZEKE electrons do not reach the detector because of their perpendicular velocity component (steradiancy discrimination).

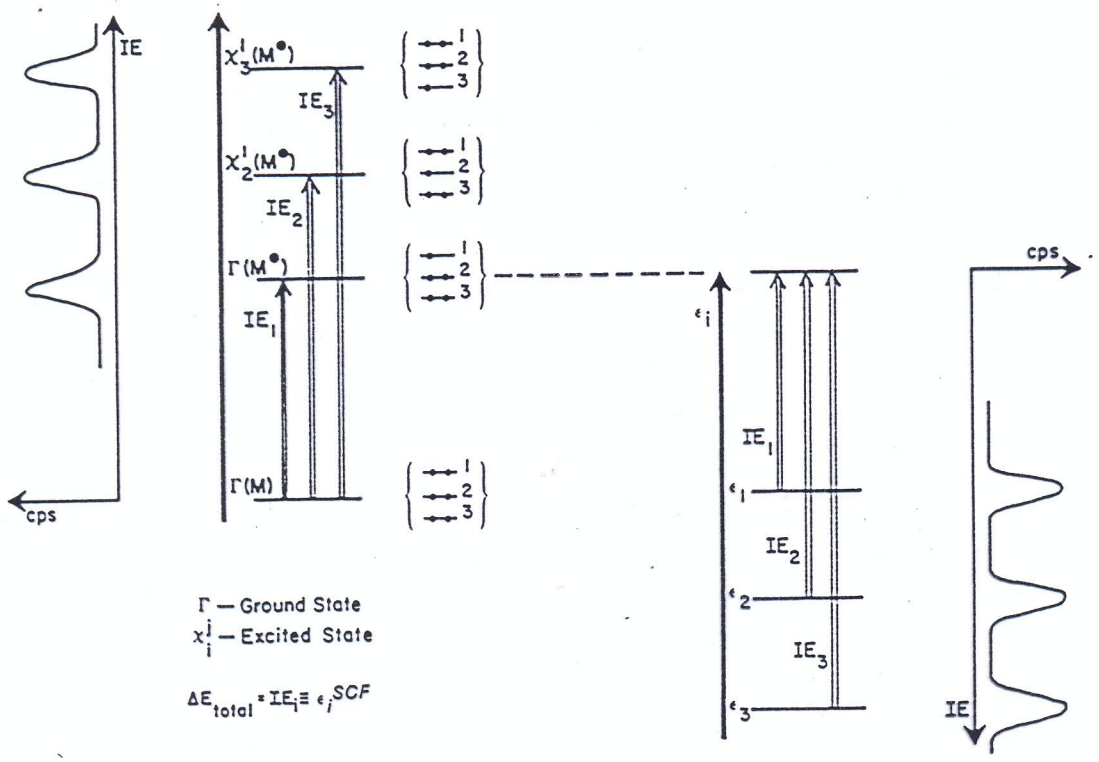

Figure 3. Koopmans' Theorem: the relationship between ionization energies and orbital energies.

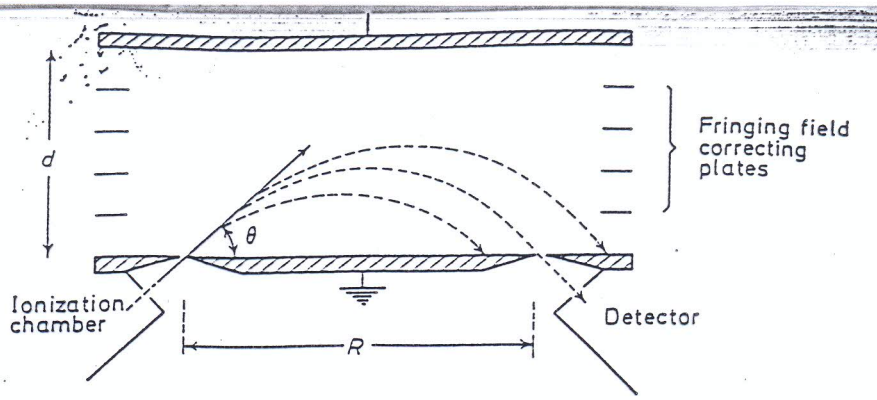

Figure 2.4. Parallel-plate electrostatic analyser in the 45 degree configuration

Electrons of energy eV_0 and mass m_e enter the field at an angle θ by passing through a slit in the plate. The initial electron velocity, v_0, is given by

$$v_0 = (2\,eV_0/m_e)^{\frac{1}{2}} \tag{2.2}$$

and its components in the two directions x and y perpendicular and parallel to the field, respectively, are

$$v_{0x} = v_0 \cos\theta \tag{2.3}$$

$$v_{0y} = v_0 \sin\theta \tag{2.4}$$

The field is of such a polarity as to decelerate the electrons in the y direction, while it has no effect on their motion in the x direction. The equations of motion are therefore

$$\frac{dv_y}{dt} = -\frac{eE}{m_e} \tag{2.5}$$

$$v_y = v_0 \sin\theta - \frac{eE}{m_e} t \tag{2.6}$$

$$y = v_0 t \sin\theta - \frac{eE}{2m_e} t^2 \tag{2.7}$$

$$x = v_0 t \cos\theta \tag{2.8}$$

The electrons follow parabolic trajectories, reaching a maximum height above the lower plate when $dy/dt = 0$, that is, when

$$t = \frac{mv_0}{eE} \sin\theta \tag{2.9}$$

The second half of the trajectory is the mirror image of the first, so that the total time until the electrons return to the lower plate is just twice this value. The distance they have then travelled in the x direction, the range, is

$$R = 2v_0 \cos\theta \frac{mv_0}{eE} \sin\theta \tag{2.10}$$

$$R = \frac{2eV_0}{eE} \sin 2\theta \tag{2.11}$$

The condition for focusing is that the range should be independent of θ, that is, $\dfrac{dR}{d\theta} = 0$. This is fulfilled at $\theta = 45$ degrees, where $\sin 2\theta = 1$.

In a practical analyser, the range, R, is fixed by the positions of the inlet and entrance slits, and different electrons are brought into focus on the exit slit by varying the electric field. If a potential, V, is applied to the plates, the field is V/d, so that the operating condition of the analyser is

$$\frac{V}{V_0} = \frac{2d}{R} \tag{2.12}$$